

Brief introduction

This is a study to investigate the potential impact of strong collective hadronization on N_μ and X_{max} . The study is performed in CONEX with the hadronic interaction models EPOS, QGSJETII and SIBYLL and uses the approach to change in a realistic way $R = E_{em}/E_{had}$ in the cascade equation.

Ratio of particle production in the micro canonical approach

The three main hadronic interaction models EPOS-LHC, QGSJETII-04 and SIBYLL2.3c are based on the string model, though the former is not completely a string model there is a pure string version available which we called EPOS-String in this analysis.

On the other hand, it is possible to obtain the particle yield coming from a different hadronization such as the one following the micro-canonical (MC) ensemble through the EPOS model, it could be then applied to all models.

The ratios between MC and each string model, R_{MC} , are shown on the first pages of the files z-alpha_ratio2-epos.ps, z-alpha_ratio2-qgsjetII.ps and z-alpha_ratio2-sibyll.ps. In the table 2 are shown the ratios used.

R_{MC}	p	π^\pm	K^\pm	K^0	π^0	n
EPOS	2.096	.855	1.512	1.500	.807	1.352
QGSJETII	2.036	.835	1.602	1.539	.766	2.192
SIBYLL	2.075	.822	1.353	1.328	.853	1.959

Table 1: Particle ratios R_{MC}

Ratio of particle production in the statistical model

The statistical model¹ applied to heavy ion collisions predicts the following ratios between particles

p/π^-	K^-/π^-	Λ/p	Ξ^-/Λ	Ω/Ξ^-
0.091	0.179	0.473	0.16	0.186

Table 2: Particle ratios in the SM

If we calculate the decay of all heavy particles, using the main decay rate

$\Lambda \rightarrow p \pi^-$	64%
$\Lambda \rightarrow n \pi^0$	36%
$\Xi^0 \rightarrow \Lambda \pi^0$	100%
$\Xi^- \rightarrow \Lambda \pi^-$	100%
$\Omega \rightarrow \Lambda K^-$	67.8%
$\Omega \rightarrow \Xi^0 \pi^-$	23.6%
$\Omega \rightarrow \Xi^- \pi^0$	8.6%

and assuming that $\Xi^0/\Lambda = \Xi^-/\Lambda$, we get the final ratios that we need to apply in the spectra

p/π^-	K^-/π^-
0.12	0.169

Unfortunately there are no information about neutral particles ratios, but we expect the same number of protons and neutrons, charged and neutral kaons, and twice charged than neutral pions, so

$$\begin{aligned} K^0/\pi^- &= K^+/\pi^- \\ n/\pi^- &= p/\pi^- \\ \pi^\pm/\pi^0 &= 1 \end{aligned}$$

As we did for the MC case, we calculate the ratios R_{SM} which indicate how much the CONEX spectra must increase to get the desire ratios between them.

R_{SM}	p	π^\pm	K^\pm	K^0	π^0	n
EPOS	1.392	.9814	1.35	1.391	.834	.950
QGSJETII	1.352	.959	1.430	1.428	.791	1.539
SIBYLL	1.378	.944	1.208	1.232	.881	1.376

Table 3: Particles ratios R_{SM}

¹<https://journals.aps.org/prc/abstract/10.1103/PhysRevC.74.034903>

Gamma spectra from π^0 spectra

To determine X_{max} CONEX uses the gamma spectra which are obtained from the neutral pions spectra. Hence, if neutral pions spectra are modified, it is necessary calculate the new gamma spectra.

Let consider that a π^0 propagate along +z axis and the angle of photon to the z axis in the rest frame is θ^* . The decay $\pi^0 \rightarrow \gamma\gamma$ is isotropic in the rest frame, so the distribution is flat as a function of $\cos \theta^*$

$$\frac{dN}{d\cos \theta^*} = \frac{1}{2} \quad (1)$$

The distribution of photon energies is,

$$\frac{dN}{dE_\gamma} = \frac{dN}{d\cos \theta^*} \frac{d\cos \theta^*}{dE_\gamma} = \frac{1}{2} \frac{d\cos \theta^*}{dE_\gamma} \quad (2)$$

In the transformation between rest and laboratory frame of the π^0 is get the energy distribution of gammas from a π^0 with momentum p_π ,

$$\frac{dN}{dE_\gamma} = \frac{2}{p_\pi} \quad (3)$$

The number of gammas with energy E_γ is,

$$N_\gamma(E_\gamma) = \int_{E_\gamma}^{\infty} \frac{2}{p_\pi} dp_\pi \quad (4)$$

The spectra in CONEX are discrete and log energy spacing, so the number of gammas in the energy range $(E_i, E_i + \Delta E_i)$ is

$$N_\gamma(E_i) \approx \sum_{j=i}^{j_{max}} \frac{2}{E_j} \Delta E_i N_\pi(E_j) \quad (5)$$

The last step is apply a scale factor to the new gamma spectra in order to have energy conservation. The gamma spectra obtained with this procedure are compare with the original spectra in the figure 1.

However, the differences at higher energies between both spectra produce a little change in X_{max} around $\pm 2 \text{ g m}^{-2}$. These differences are energy shower and mass composition dependent and can be parameterize by $\Delta X_{max}(E, \theta)$. For inclined showers the linear interpolations between $\log E=14$ and $\log E=19$ are:

Model	Primary	$\Delta X_{max}(E, \theta = 67^\circ)$
EPOS	p	-0.052(logE-14)+0.58
EPOS	Fe	-0.038(logE-14)+0.60
QGSJETII	p	1.9
QGSJETII	Fe	0.142(logE-14)+1.12
SIBYLL	p	-0.282(logE-14)+1.24
SIBYLL	Fe	-0.022(logE-14)+1.34

These corrections are applied in all shower simulations.

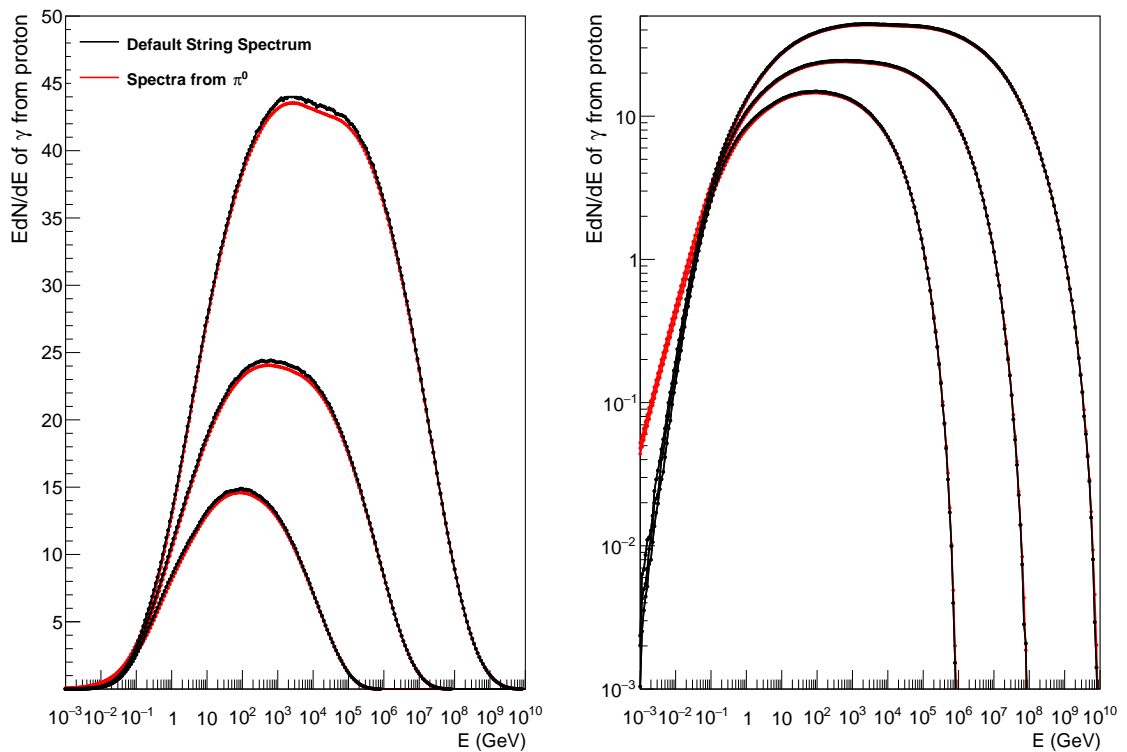


Figure 1: Gamma spectrum calculated from π^0 in linear scale (left) and log scale (right)

How transfers increase with energy

The goal of this work is change the CONEX spectra from string (the default spectra) to MC or SM and analyze their impact in the muon number. However these changes must not be applied for all energies since there are constraints from experimental data. For this reason, the changes are implemented from an initial interacting energy and increase linearly with the logarithm of the energy up to a given energy E_{int} , from where the increase is constant or uniform with the energy. The figure 2 compare the linear and uniform increase when both start at the same energy.

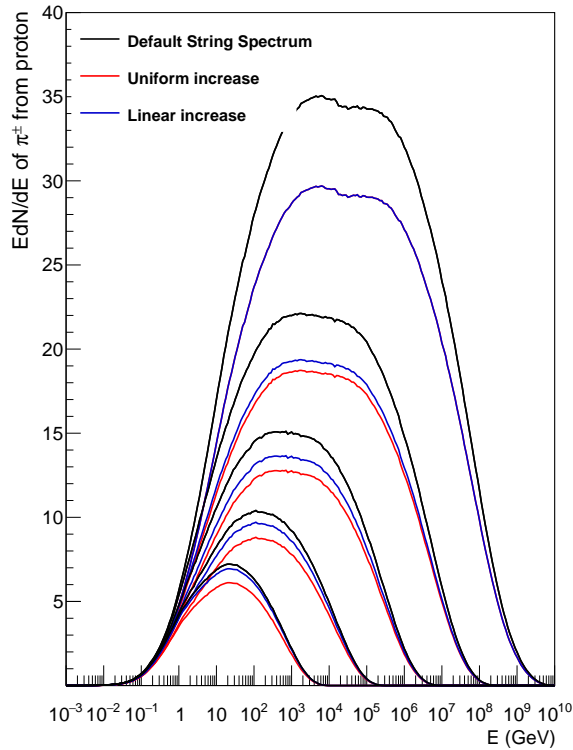


Figure 2: Uniform and linear increase. For the most energetic spectrum both line overlap

Application of R_{MC} and R_{SM} in the CONEX spectra

Both ratios are applied to the spectra following three mandatory rules. The first one is conserve energy after the changes in all cases. The second one is not change the leading particle part of the spectra, so the spectra with leading particle are used as the source of energy for the other spectra. After all the changes these spectra should change as if the ratio had been apply without change the leading particle part. The last one is transfer energy between particles only bin by bin.

Here are shown the spectra for proton-air interaction in the three models with a linear increase of changes, but in the file RatioAnalysis-All_Spectra.pdf are all the spectra of all interaction.

EPOS - Proton+air interaction

Kaons and pions spectra are scaled by their respective R_{MC} and R_{SM} taking/giving the energy from/to protons and neutrons bin by bin in the whole energy range.

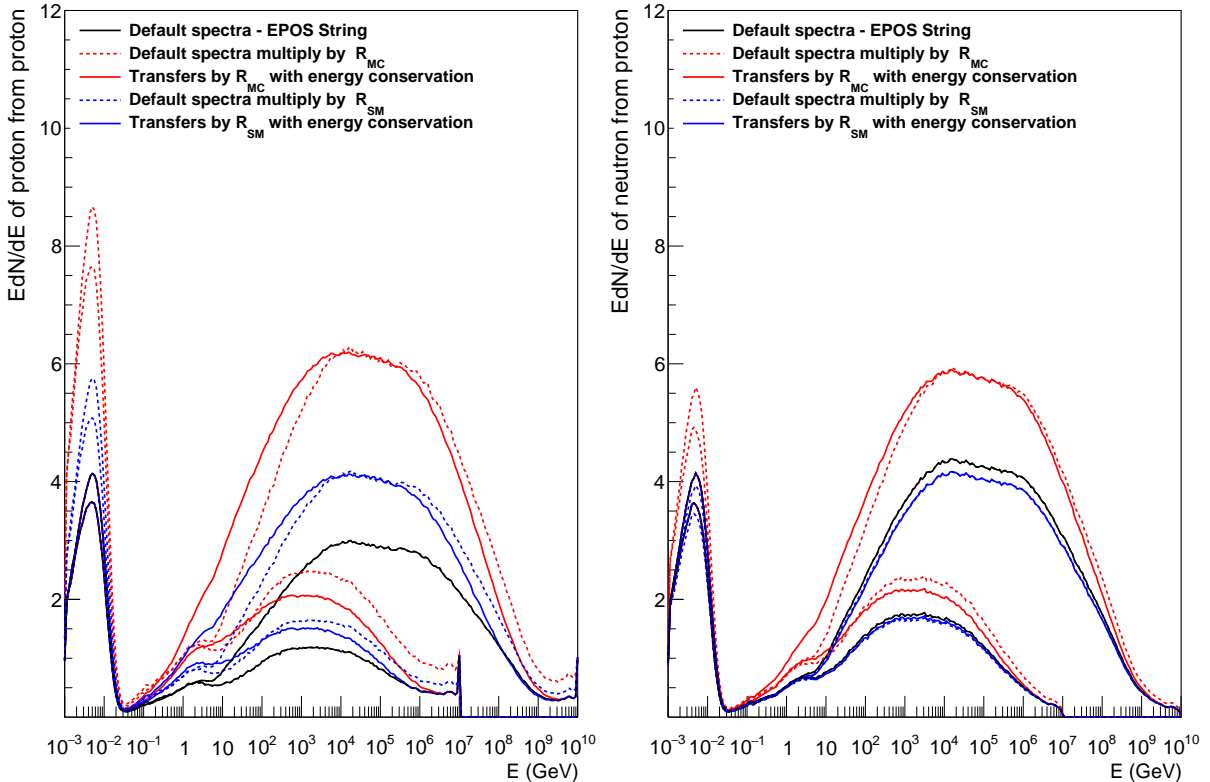


Figure 3: Spectrum of proton (left) and neutron (right) for p+air interaction at two different energies applying R_{MC} and R_{SM} and energy conservation.

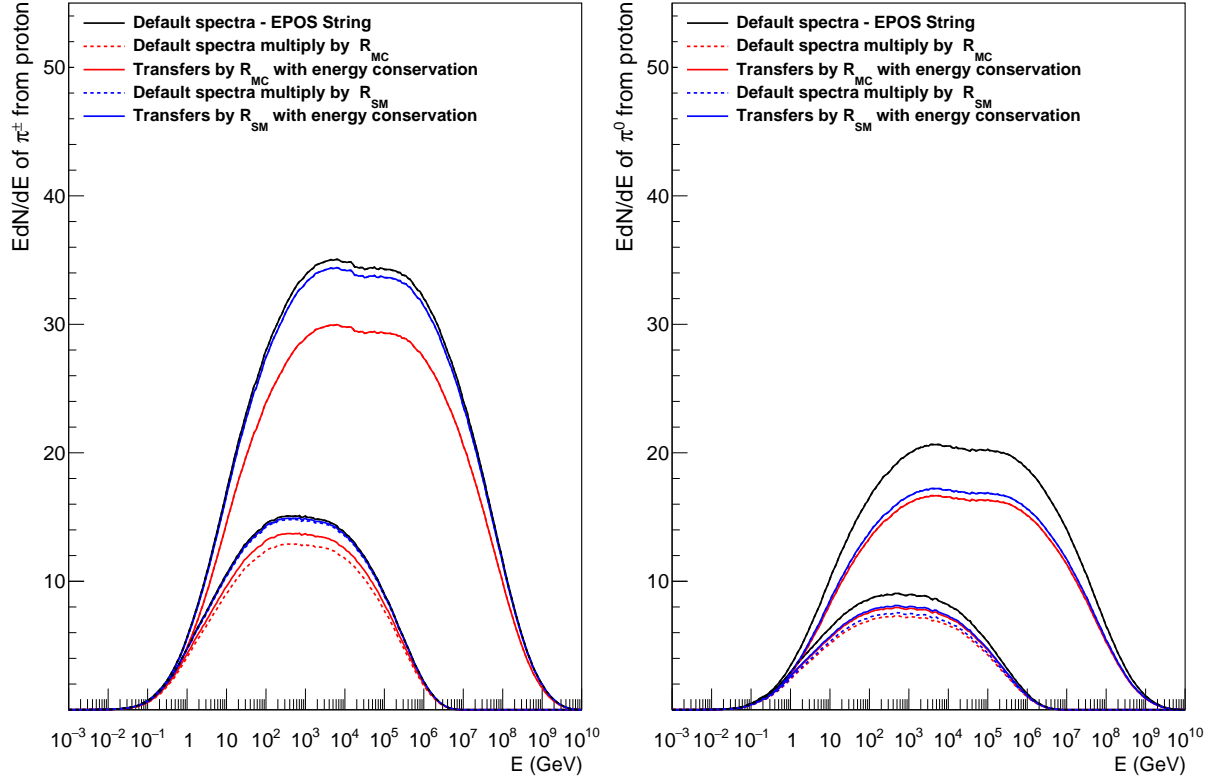


Figure 4: Spectrum of π^\pm (left) and π^0 (right) for p+air interaction at two different energies applying R_{MC} and R_{SM} and energy conservation, in this case some lines overlap

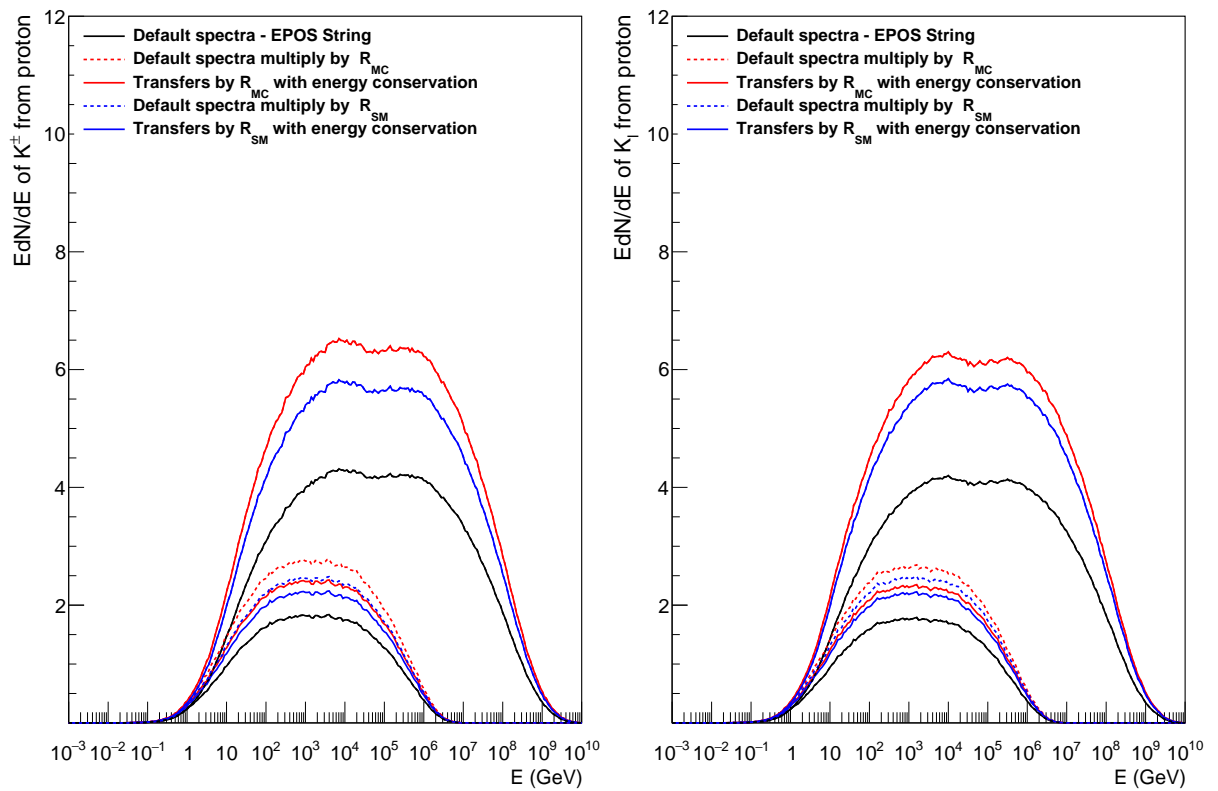


Figure 5: Spectrum of K^\pm (left) and K_l (right) for p+air interaction at two different energies applying R_{MC} and R_{SM} and energy conservation, in this case some lines overlap

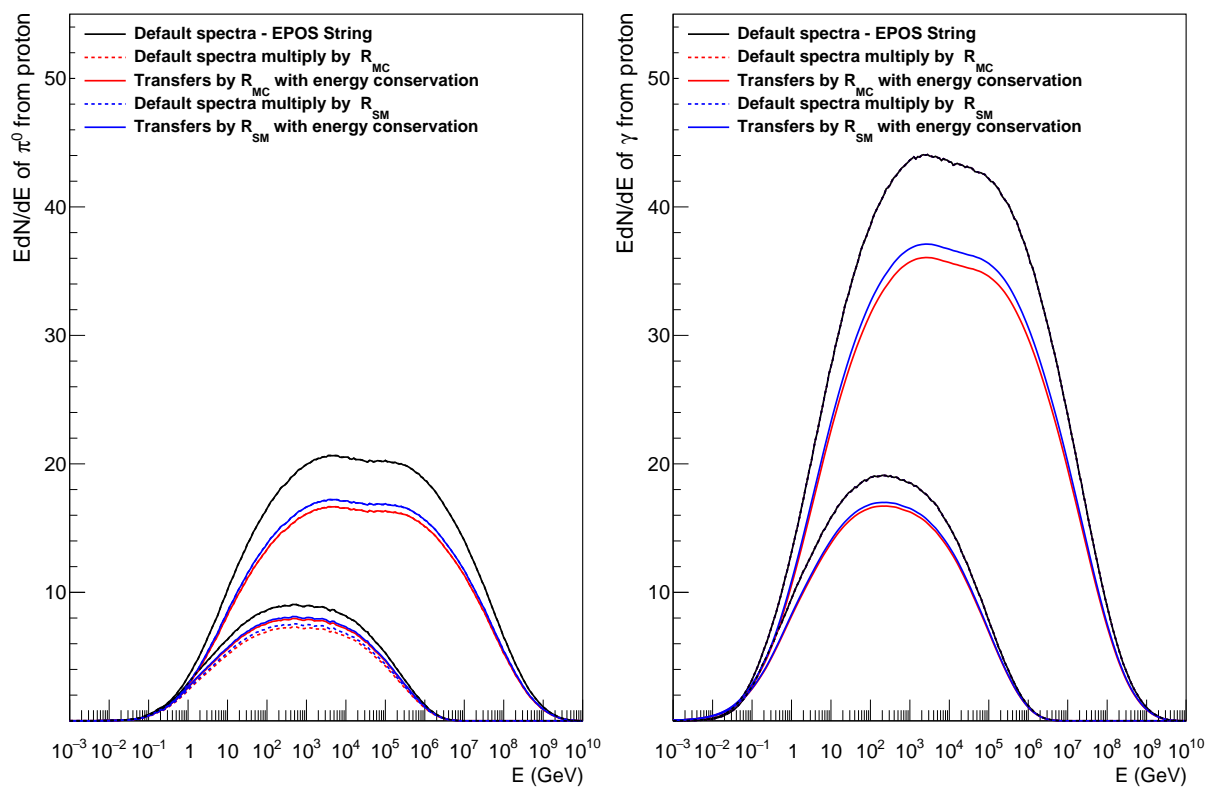


Figure 6: Spectrum of π^0 and gammas for p+air interaction at two different energies applying R_{MC} and R_{SM} and energy conservation, in this case some lines overlap

QGSJETII - Proton+air interaction

Kaons and pions spectra are scaled by their respective R_{MC} and R_{SM} taking/giving the energy from/to protons and neutrons bin by bin in the whole energy range.

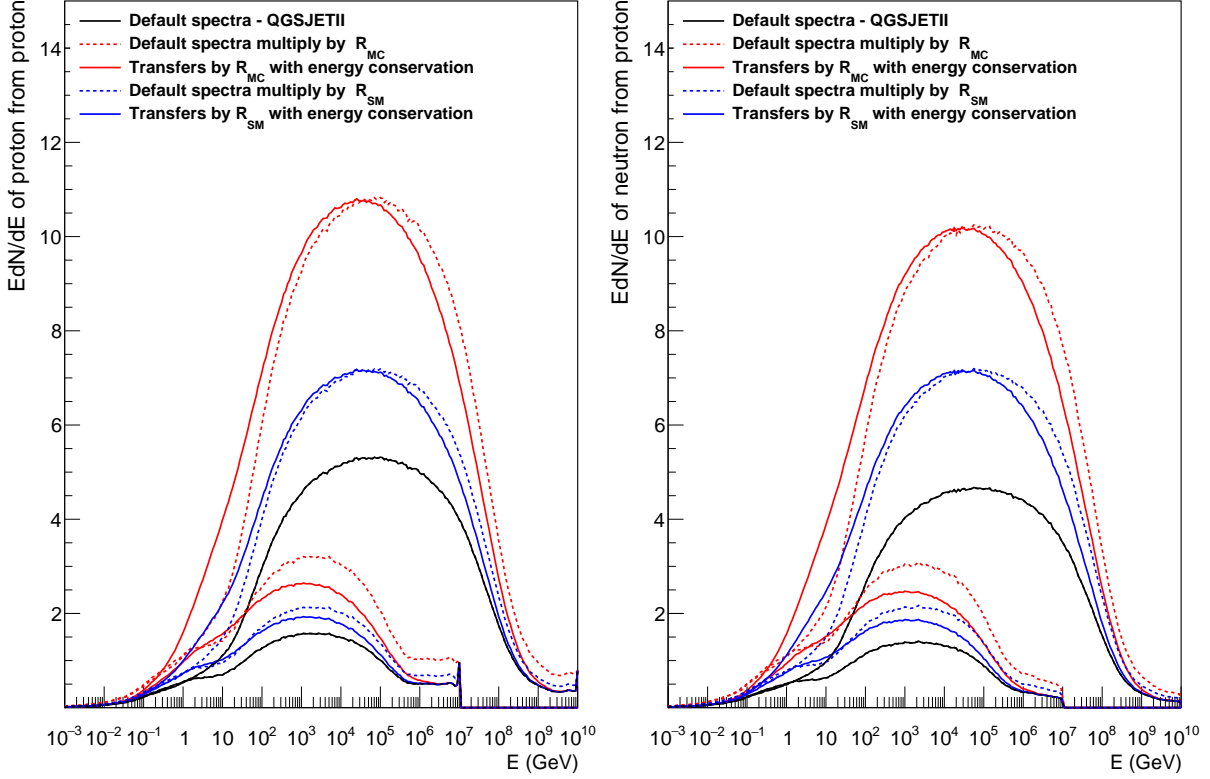


Figure 7: Spectrum of proton (left) and neutron (right) for p+air interaction at two different energies applying R_{MC} and R_{SM} and energy conservation

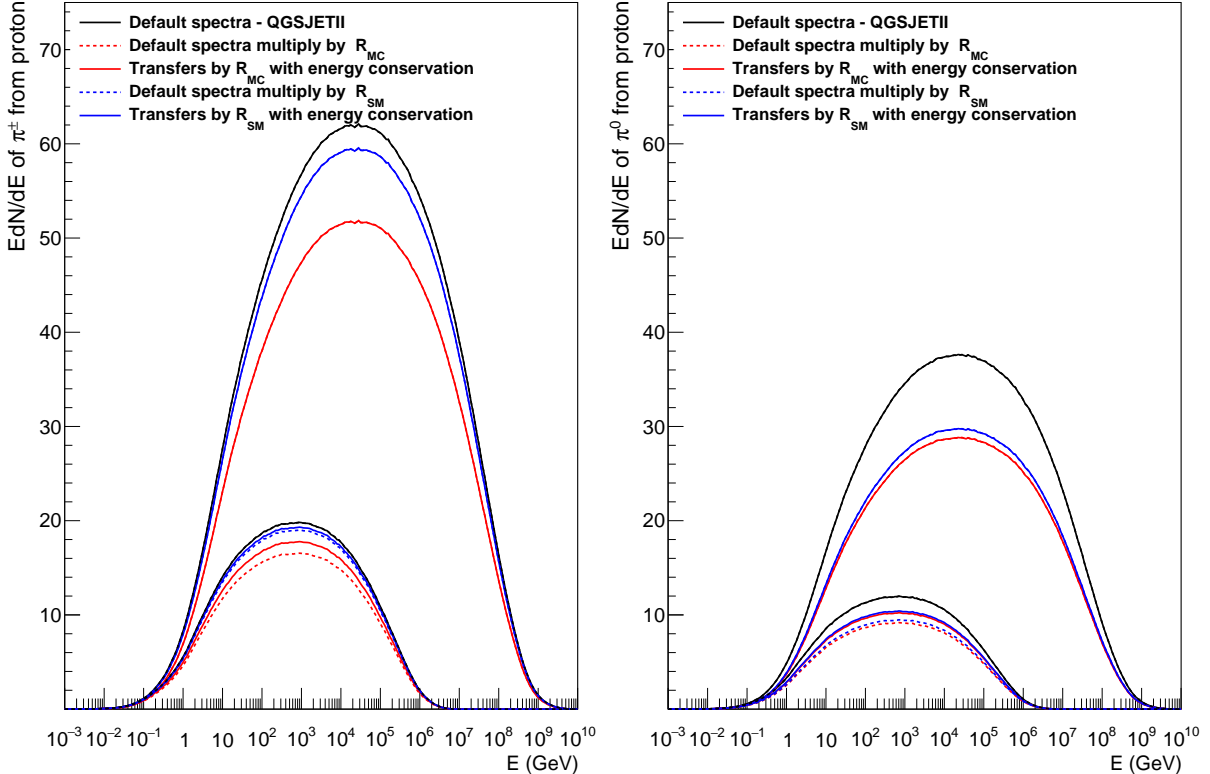


Figure 8: Spectrum of π^\pm (left) and π^0 (right) for p+air interaction at two different energies applying R_{MC} and R_{SM} and energy conservation, in this case some lines overlap

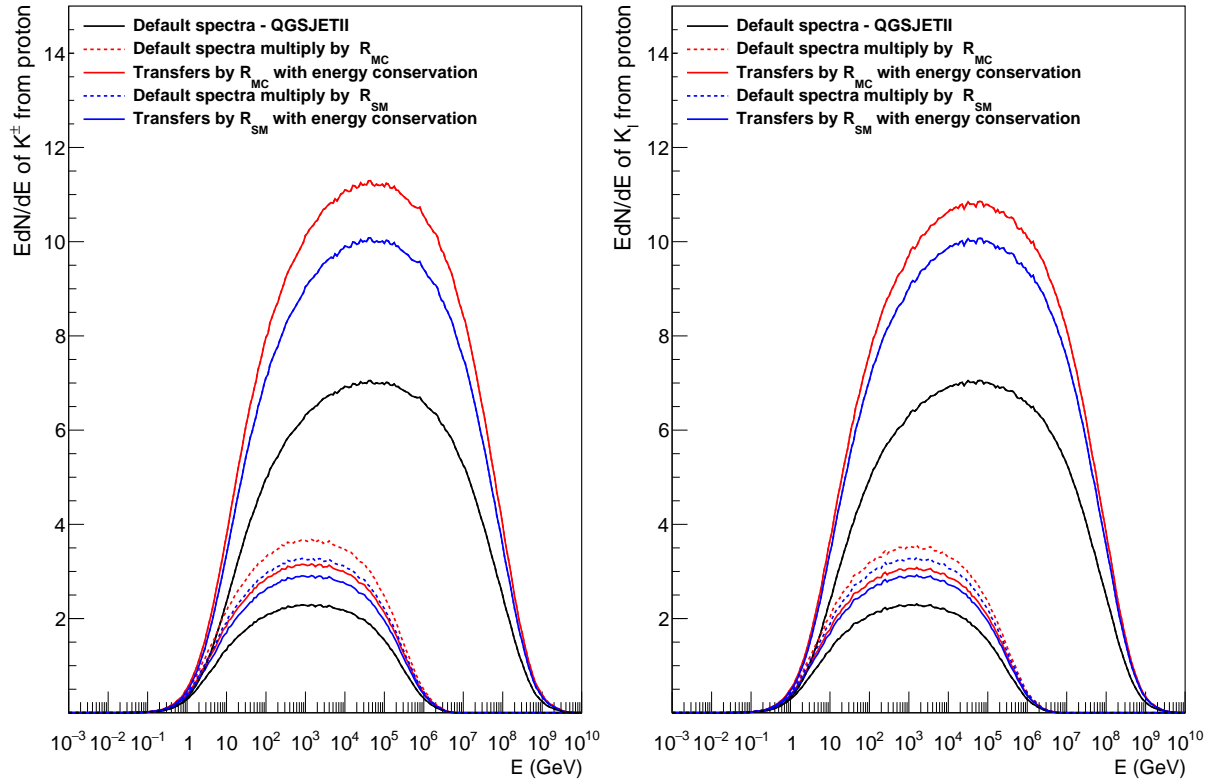


Figure 9: Spectrum of K^\pm (left) and K_l (right) for p+air interaction at two different energies applying R_{MC} and R_{SM} and energy conservation, in this case some lines overlap

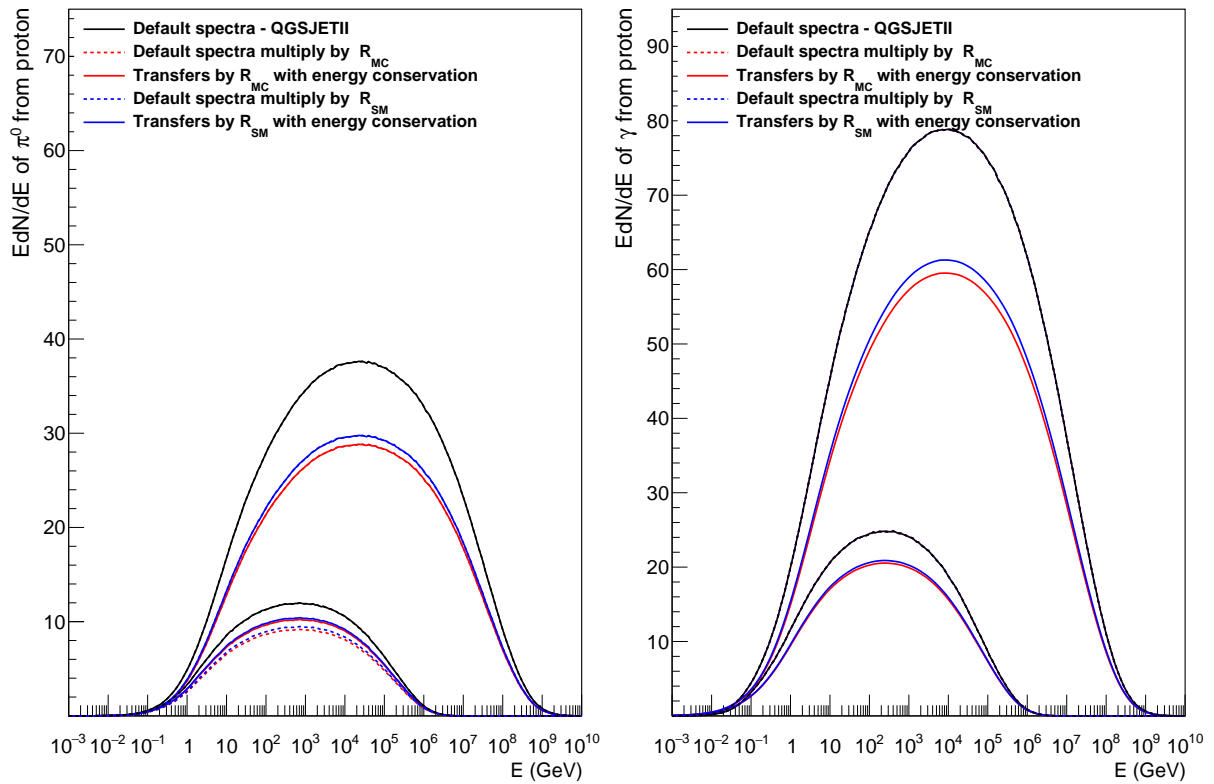


Figure 10: Spectrum of π^0 and gammas for p+air interaction at two different energies applying R_{MC} and R_{SM} and energy conservation, in this case some lines overlap

SIBYLL - Proton+air interaction

Kaons and pions spectra are scaled by their respective R_{MC} and R_{SM} taking/giving the energy from/to protons and neutrons bin by bin in the whole energy range.

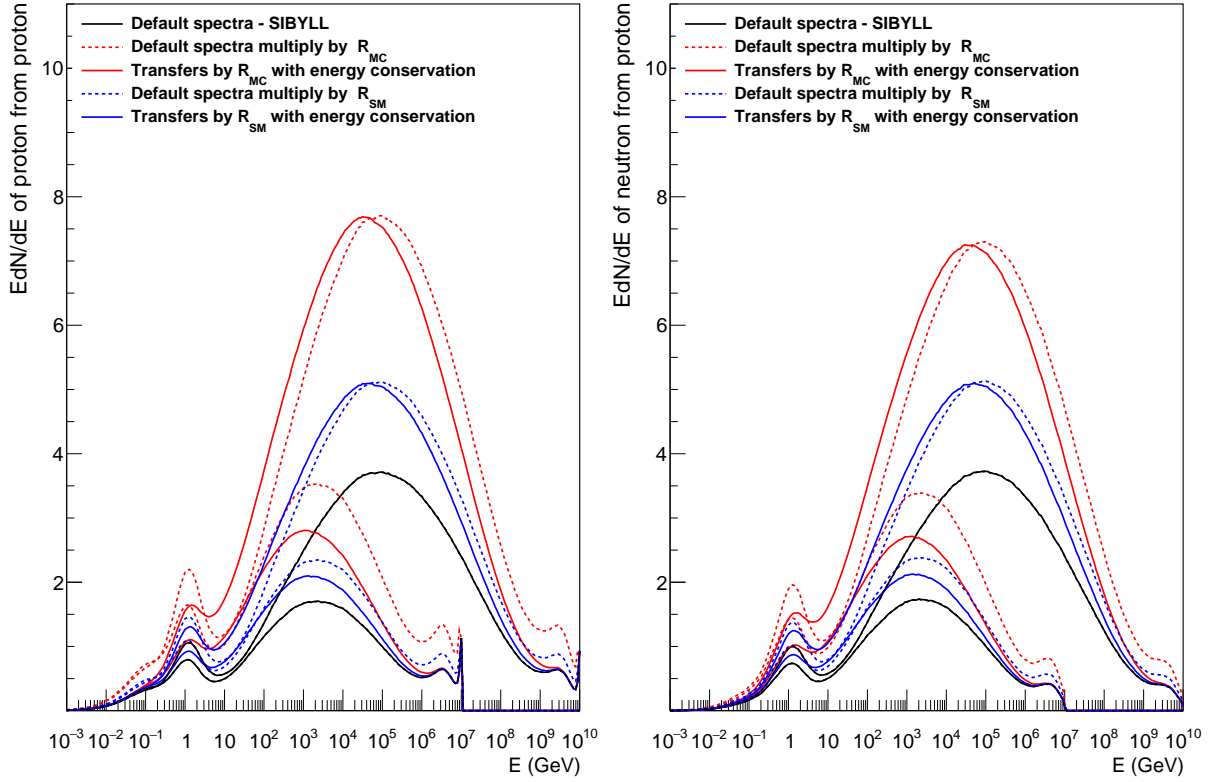


Figure 11: Spectrum of proton (left) and neutron (right) for p+air interaction at two different energies applying R_{MC} and R_{SM} and energy conservation

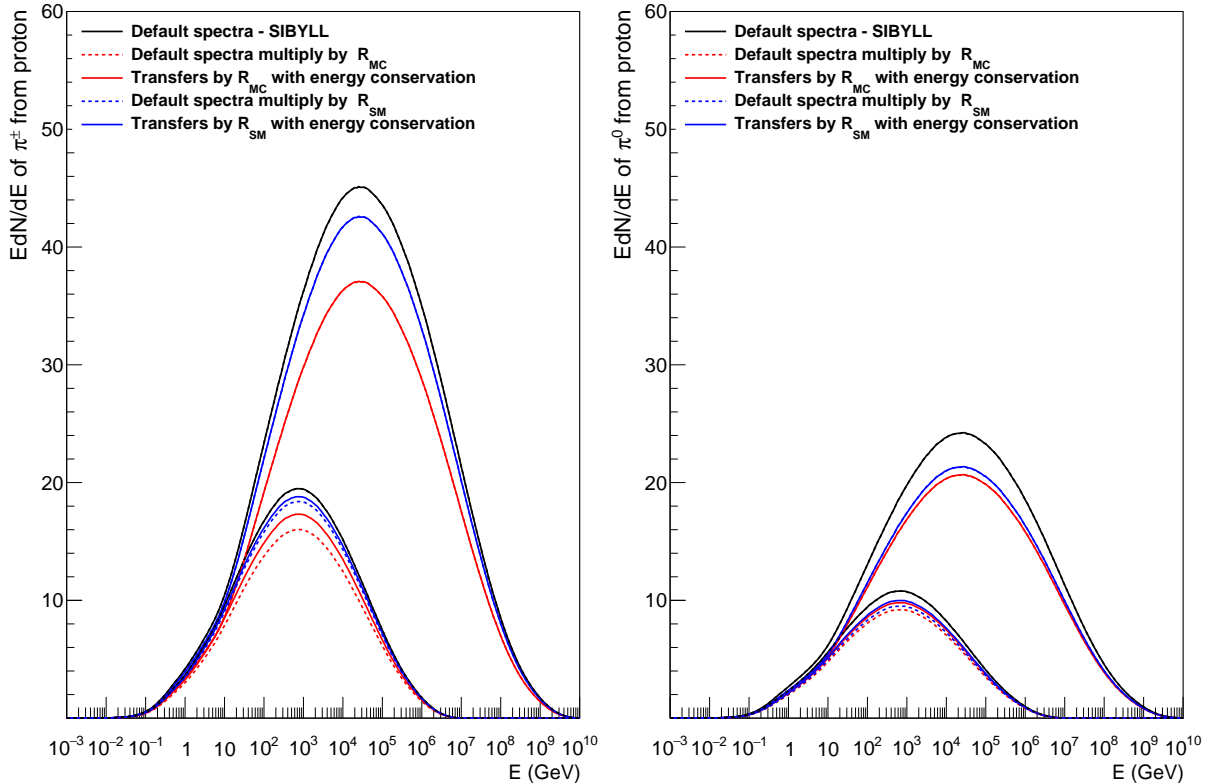


Figure 12: Spectrum of π^\pm (left) and π^0 (right) for p+air interaction at two different energies applying R_{MC} and R_{SM} and energy conservation, in this case some lines overlap

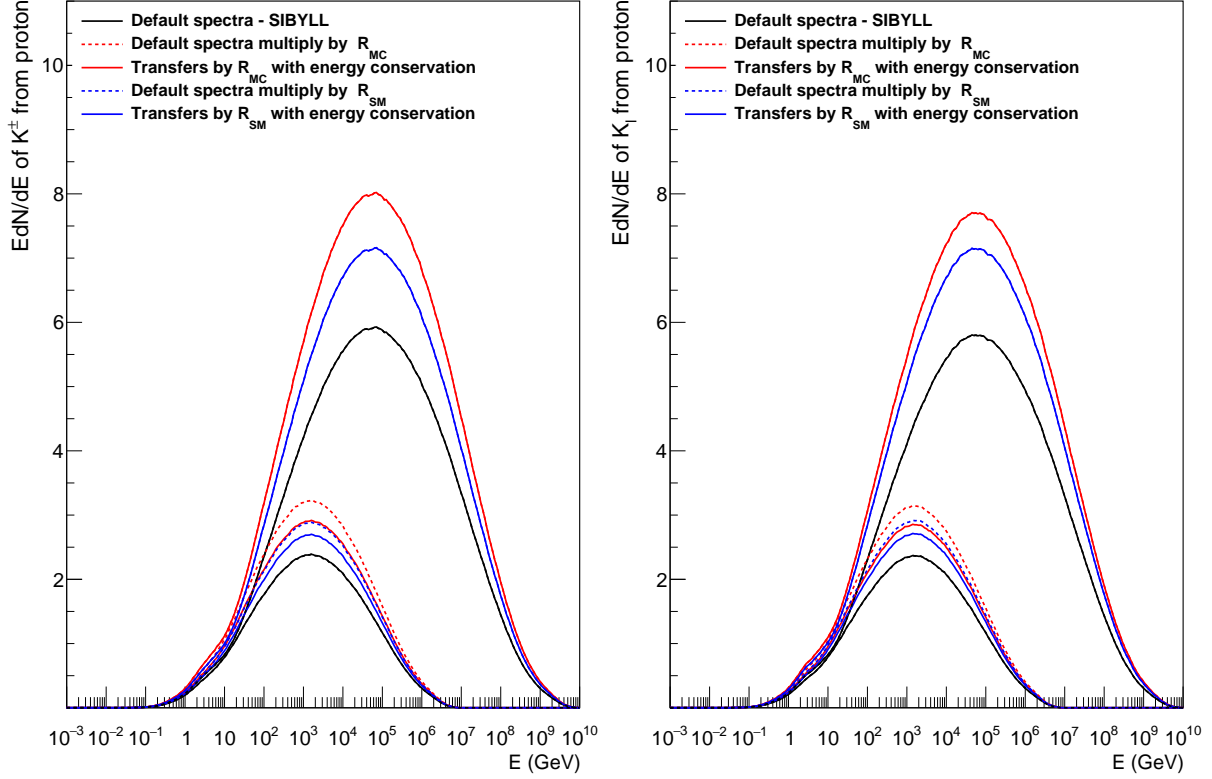


Figure 13: Spectrum of K^\pm (left) and K_l (right) for p+air interaction at two different energies applying R_{MC} and R_{SM} and energy conservation, in this case some lines overlap

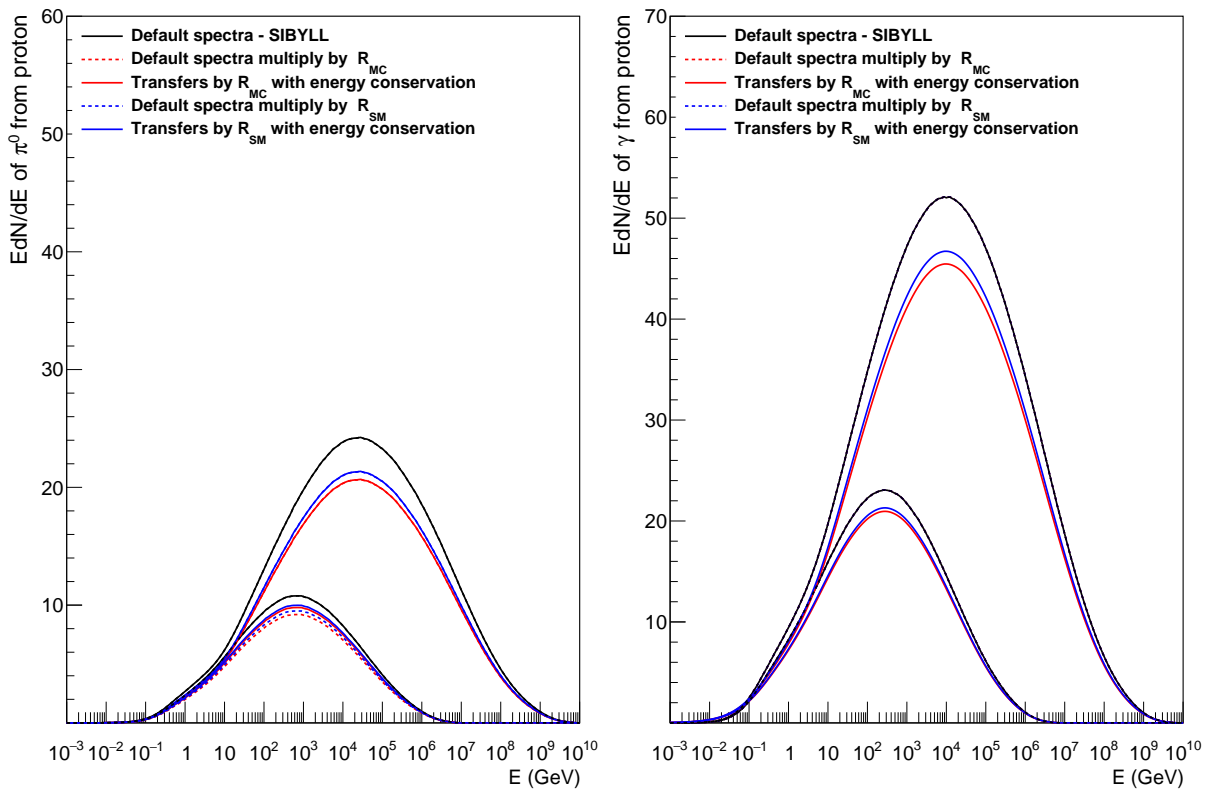


Figure 14: Spectrum of π^0 and gammas for p+air interaction at two different energies applying R_{MC} and R_{SM} and energy conservation, in this case some lines overlap

Muon numbers

Proton and iron showers at 1425 m a.s.l. with $\theta = 67^\circ$ are simulated in CONEX using the cascade equations analysis from the first interaction. The number of muons over 0.3 GeV are analyzed when different fractions of R_{MC} and R_{SM} are applied with a log linear increase with the energy up to an energy E_{int} . When E_{int} is lower than the maximum energy, transfers for larger energies are uniform or constant. All transfers start at 100 GeV.

EPOS

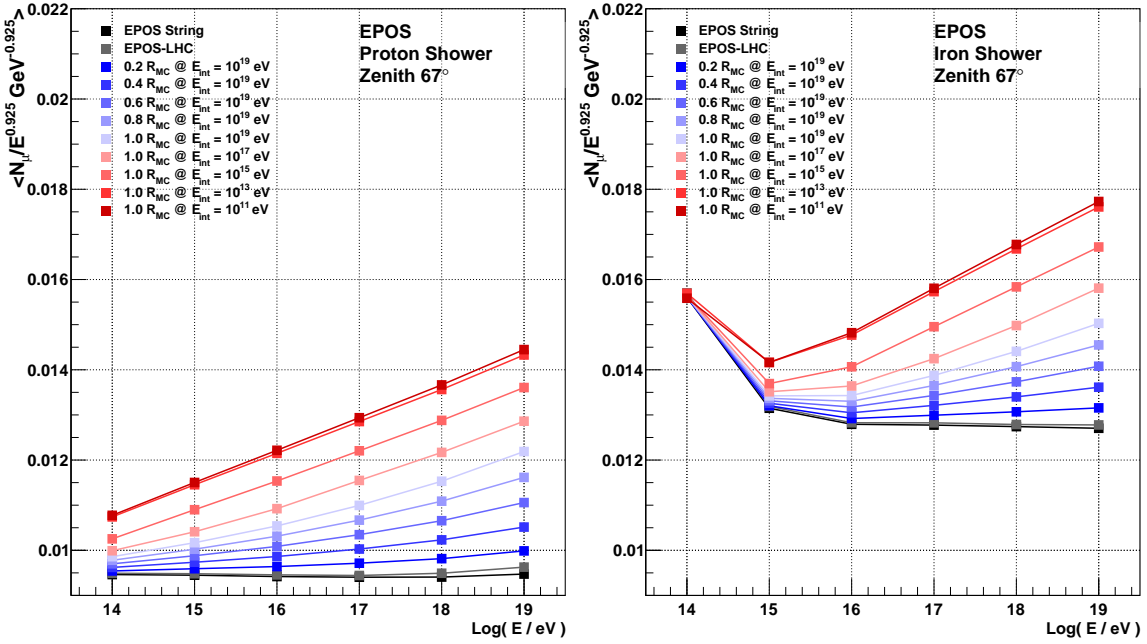


Figure 15: Muon number using R_{MC} - EPOS

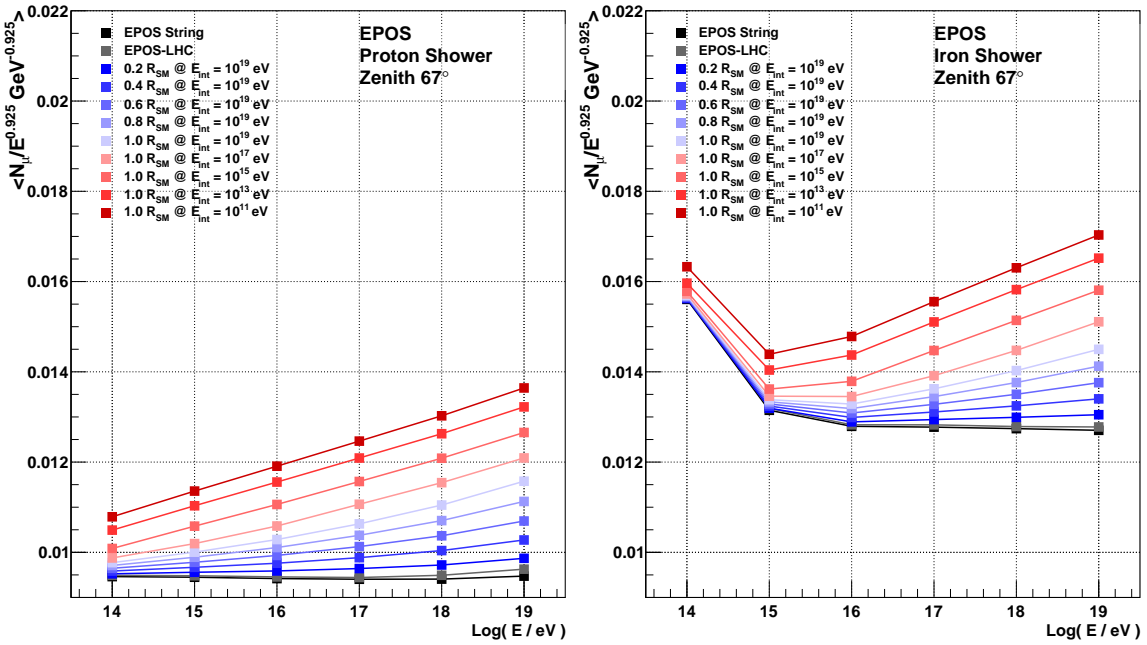


Figure 16: Muon number using R_{SM} - EPOS

QGSJETT-II

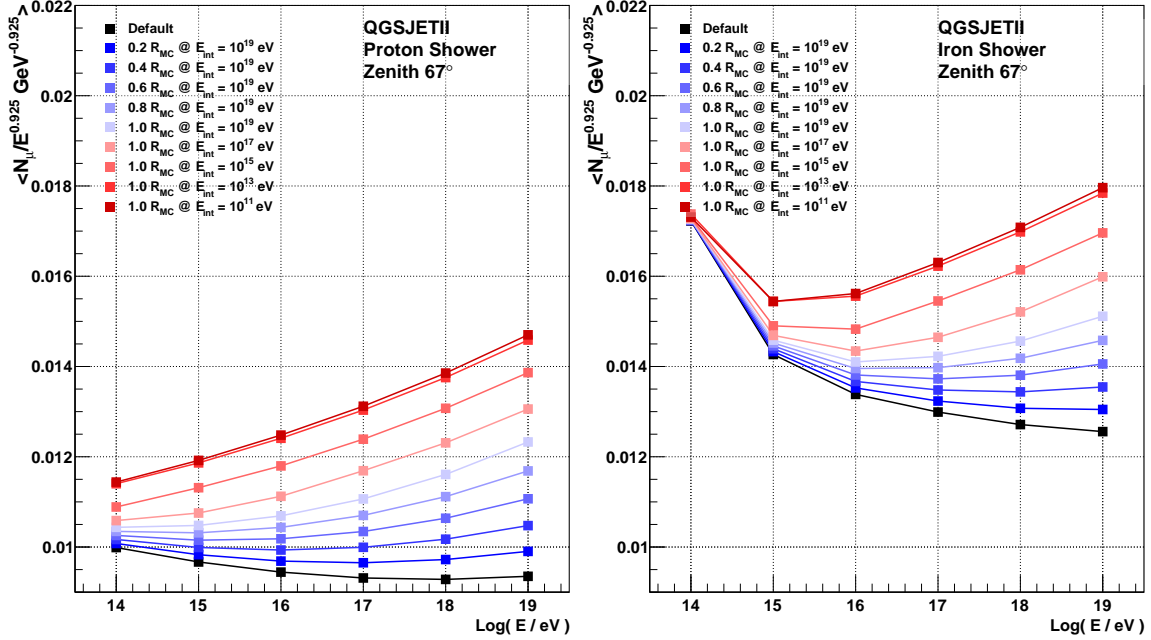


Figure 17: Muon number using R_{MC} - QGSJETII

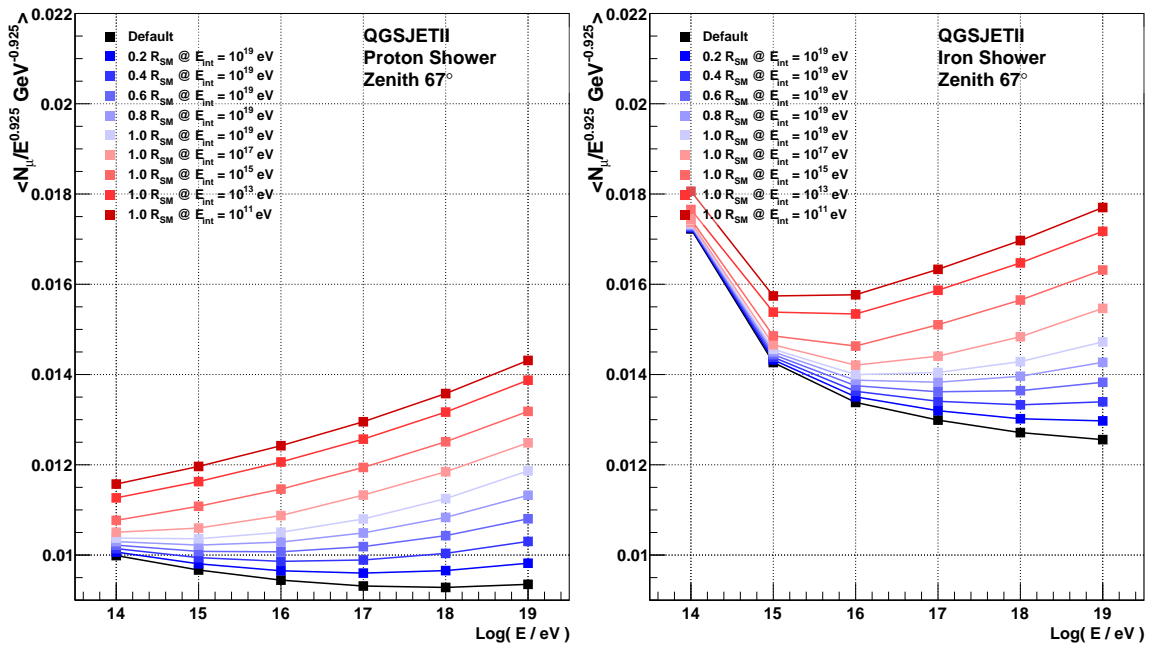


Figure 18: Muon number using R_{SM} - QGSJETII

SIBYLL

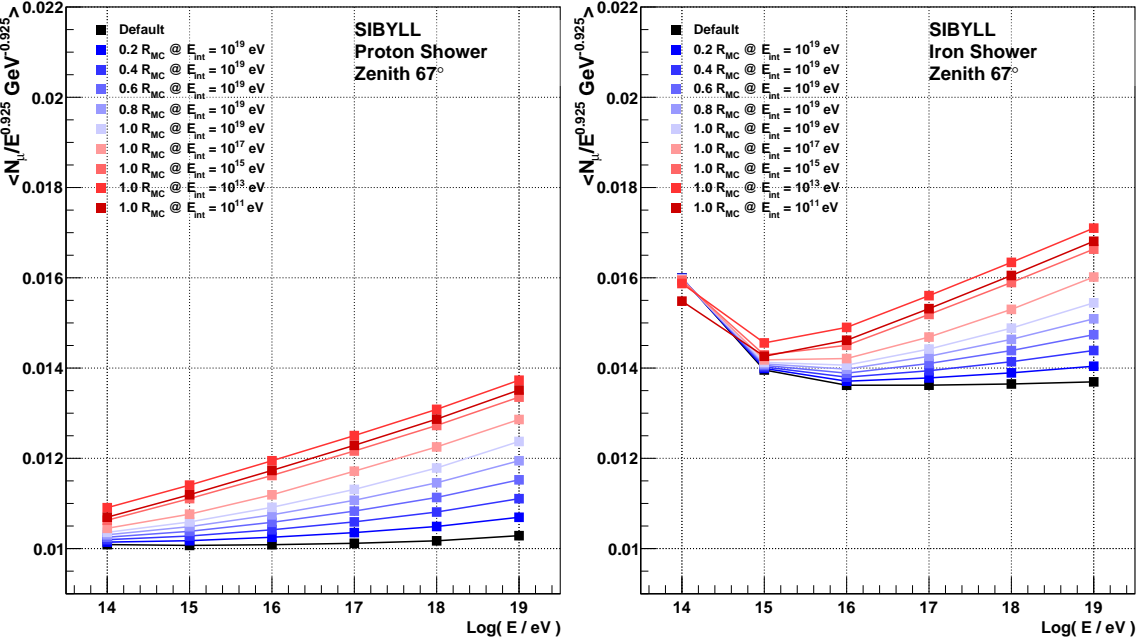


Figure 19: Muon number using R_{MC} - SIBYLL

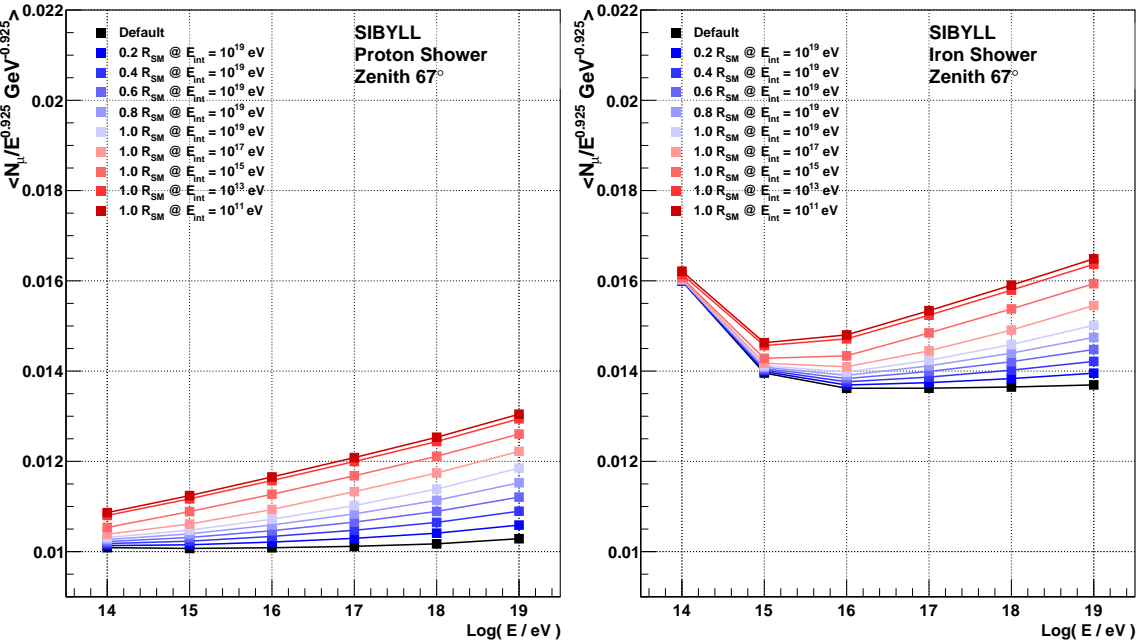


Figure 20: Muon number using R_{SM} - SIBYLL

Xmax

The figures 25 and 29 show how change the Xmax in transfers considered on the above sections.

EPOS

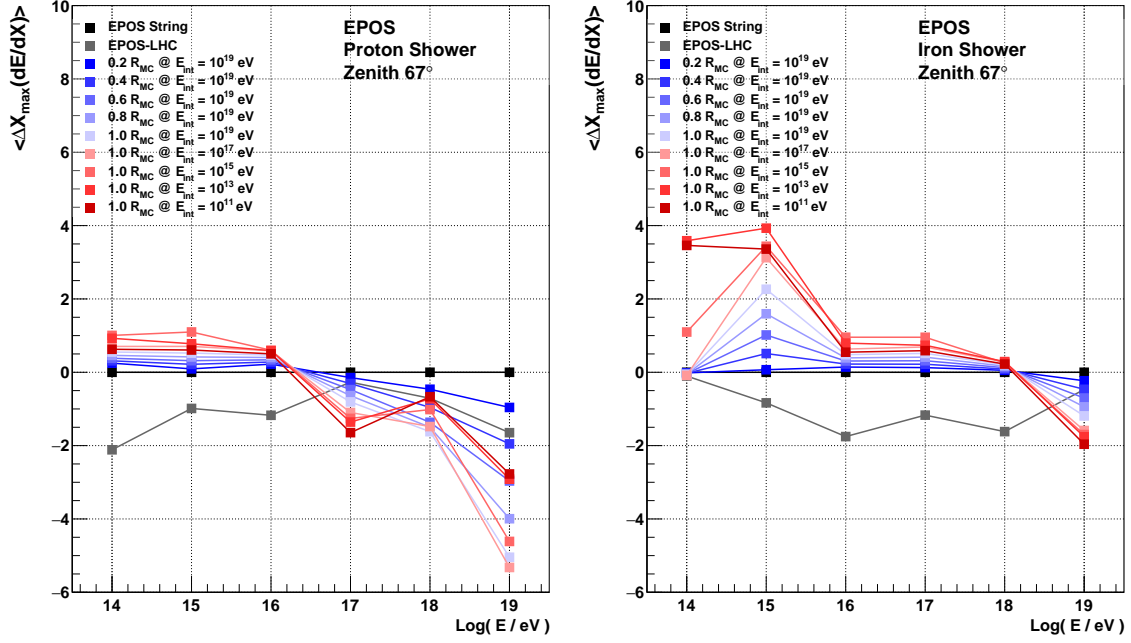


Figure 21: ΔX_{\max} using R_{MC}

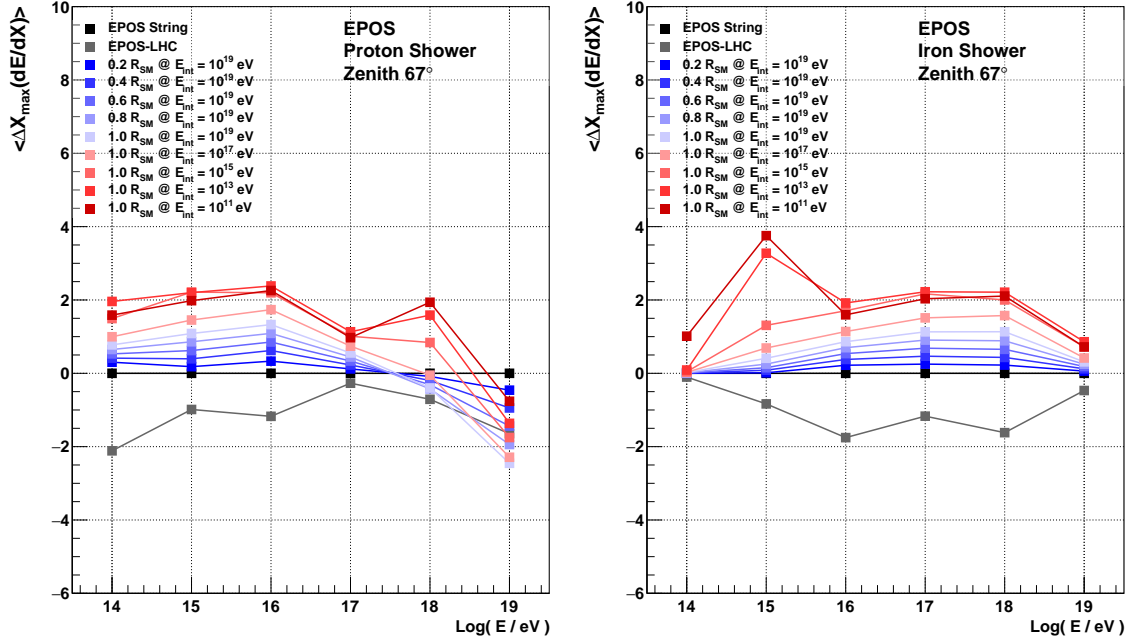


Figure 22: ΔX_{\max} using R_{SM}

QGSJETT-II

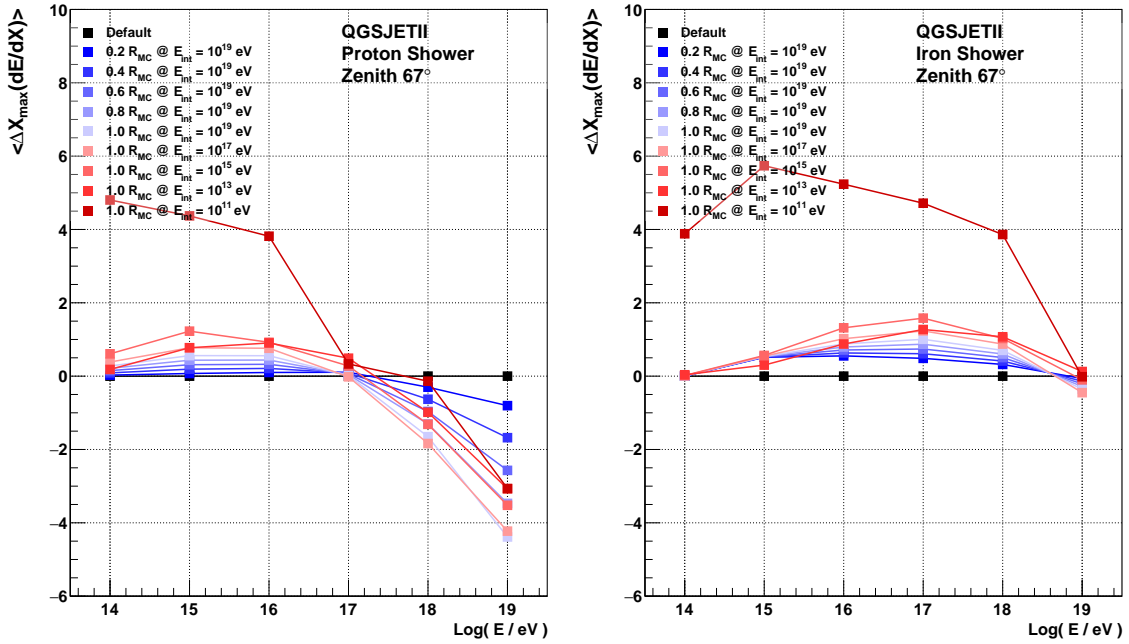


Figure 23: ΔX_{max} using R_{MC}

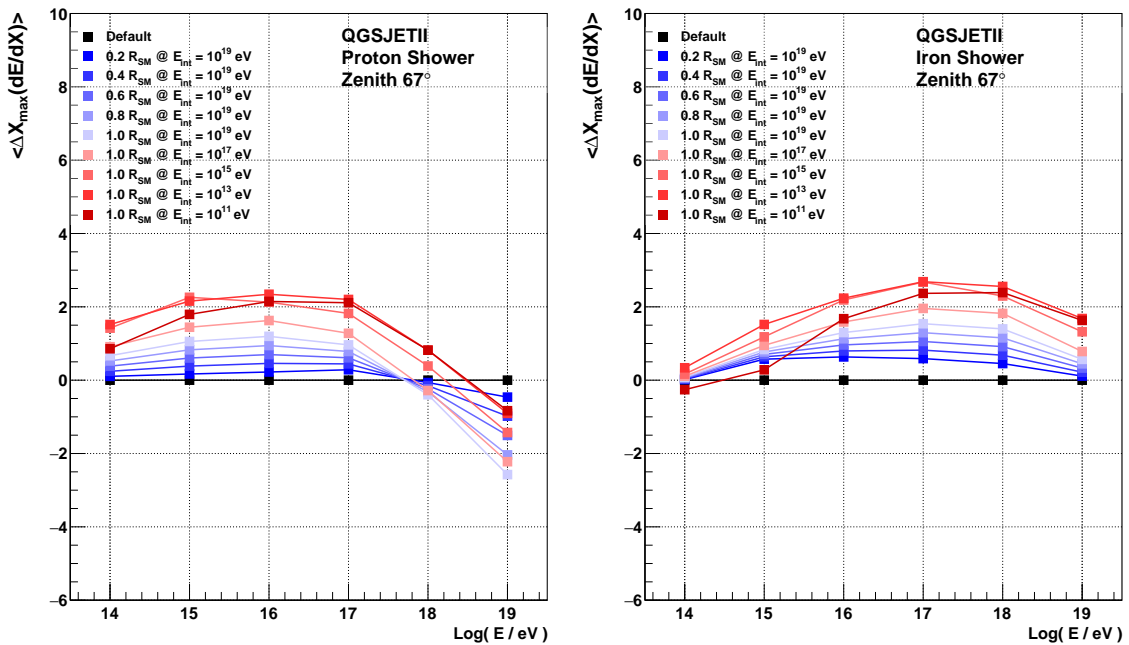


Figure 24: ΔX_{max} using R_{SM}

SIBYLL

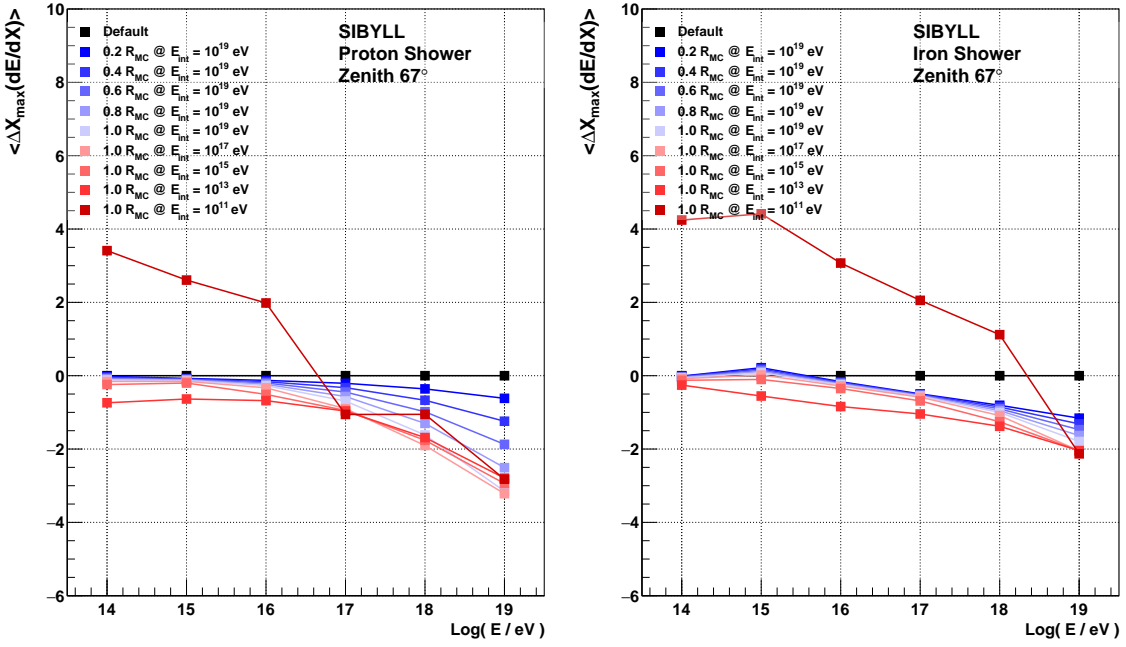


Figure 25: ΔX_{max} using R_{MC}

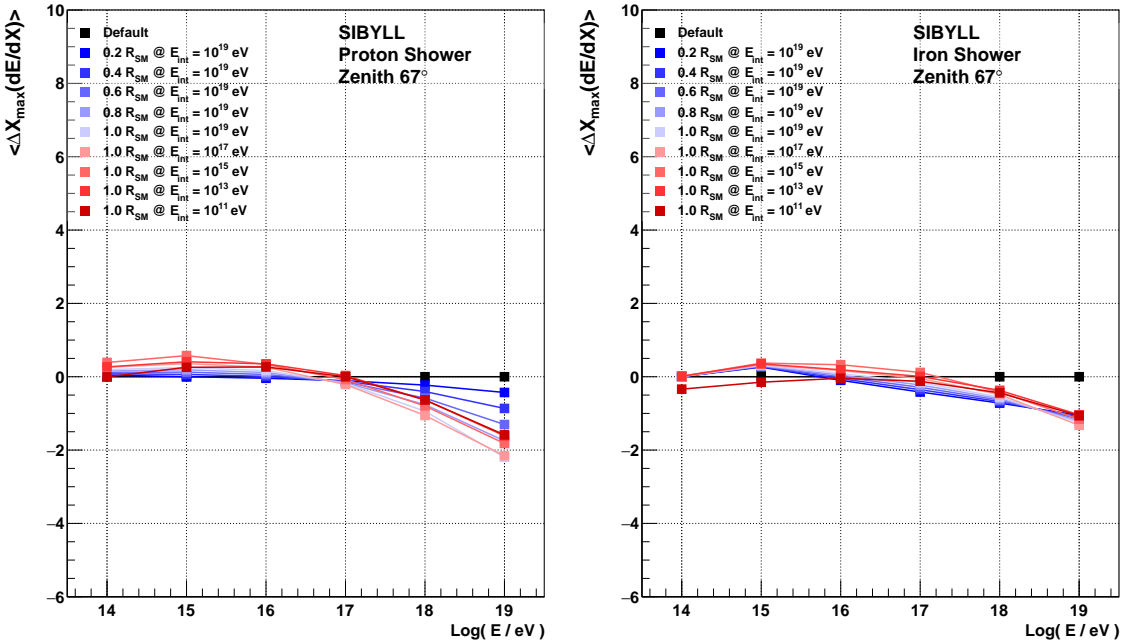


Figure 26: ΔX_{max} using R_{SM}

Nmu vs Xmax

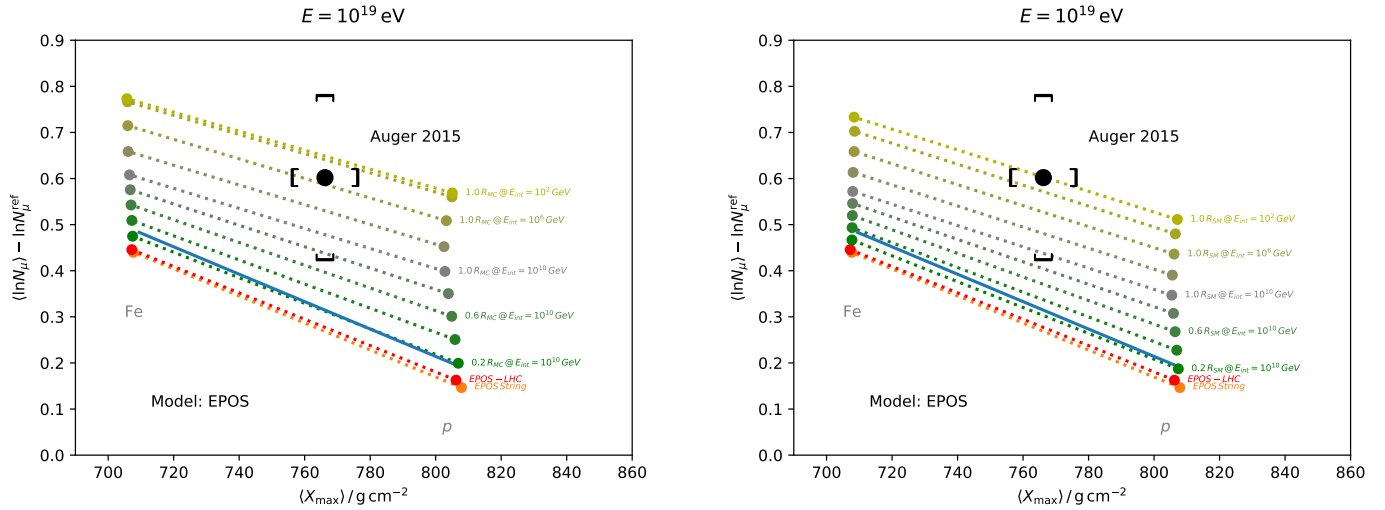


Figure 27: Xmax for different values of R_{MC} in vertical showers of proton (left) and iron (right), both with an uniform increment of transfers with energy

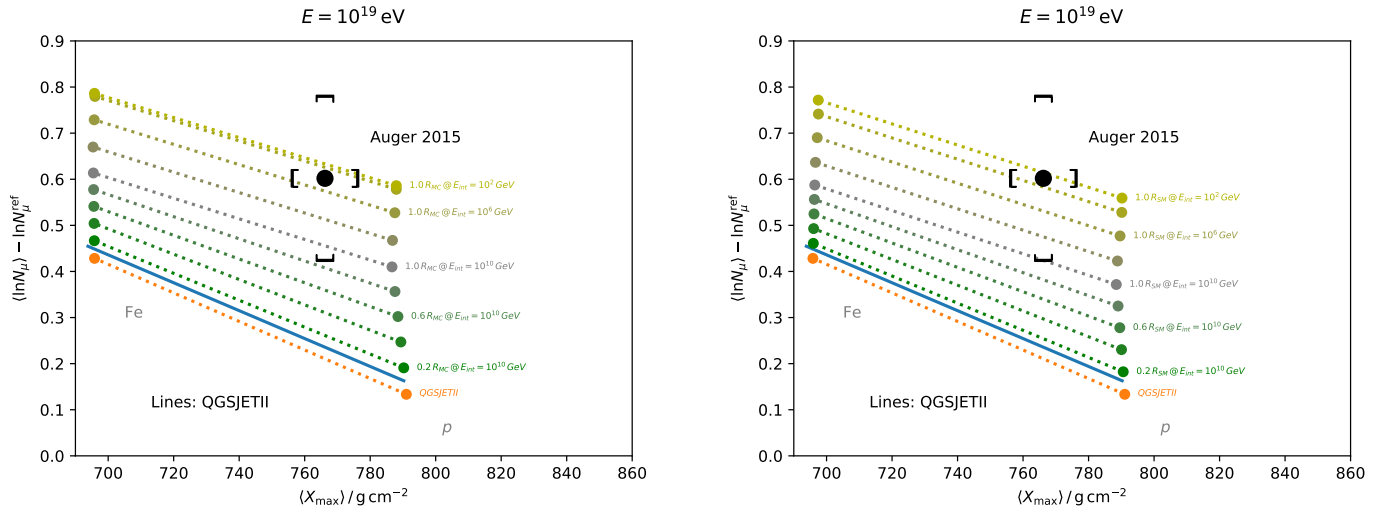


Figure 28: Xmax for different values of R_{MC} in vertical showers of proton (left) and iron (right), both with an uniform increment of transfers with energy

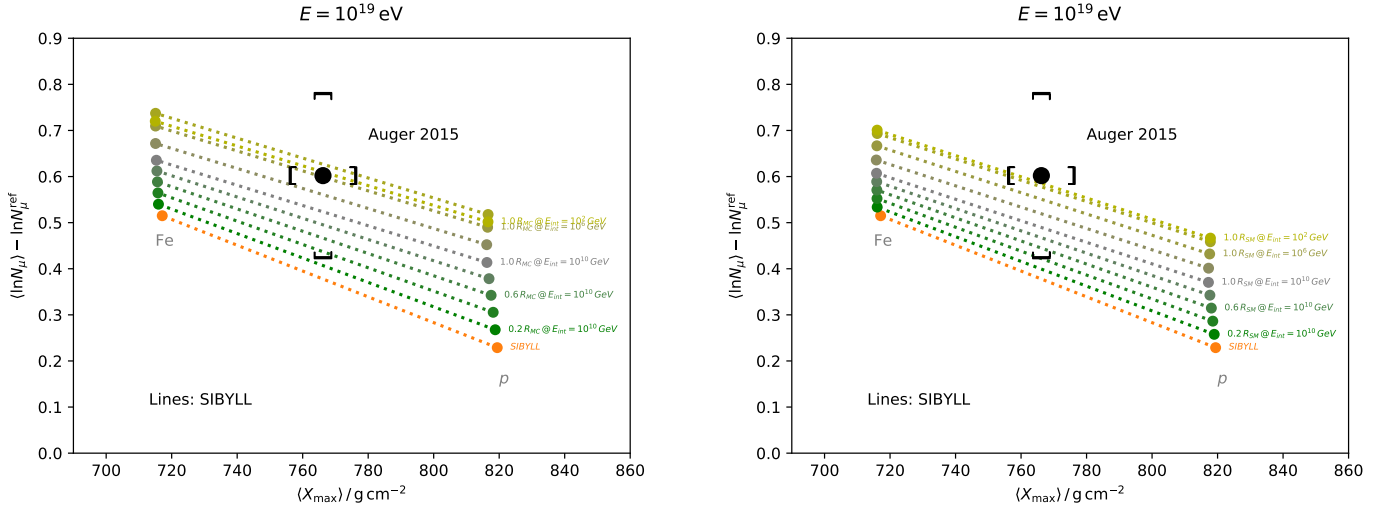


Figure 29: X_{\max} for different values of R_{MC} in vertical showers of proton (left) and iron (right), both with an uniform increment of transfers with energy

Muon number - Vertical Showers

Same analysis as before but for vertical showers

EPOS

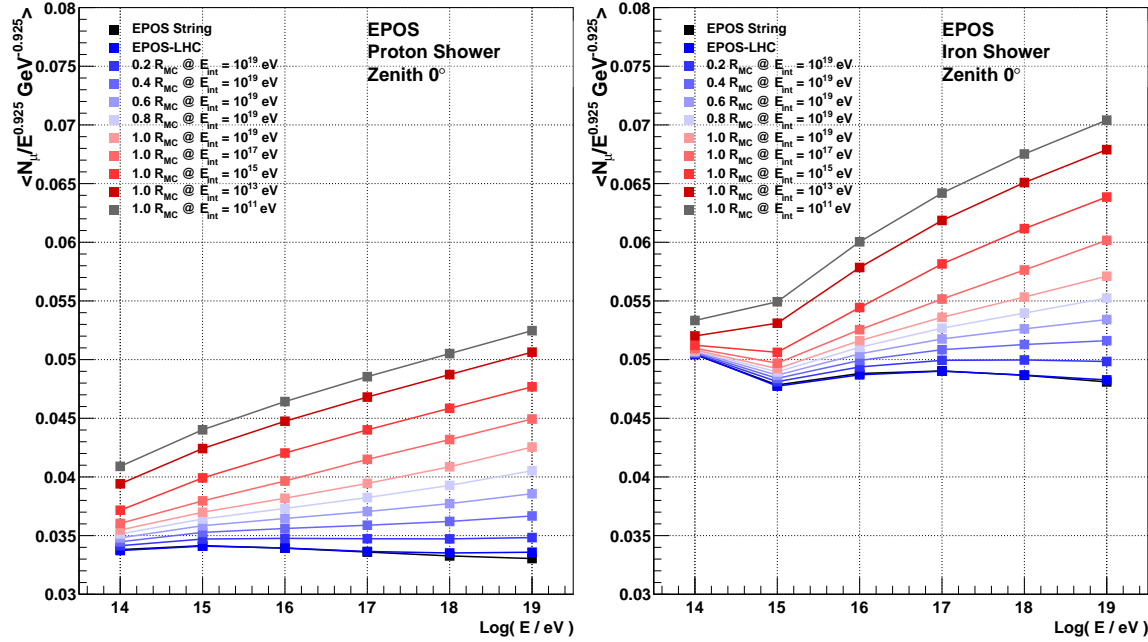


Figure 30: Muon number using R_{MC}

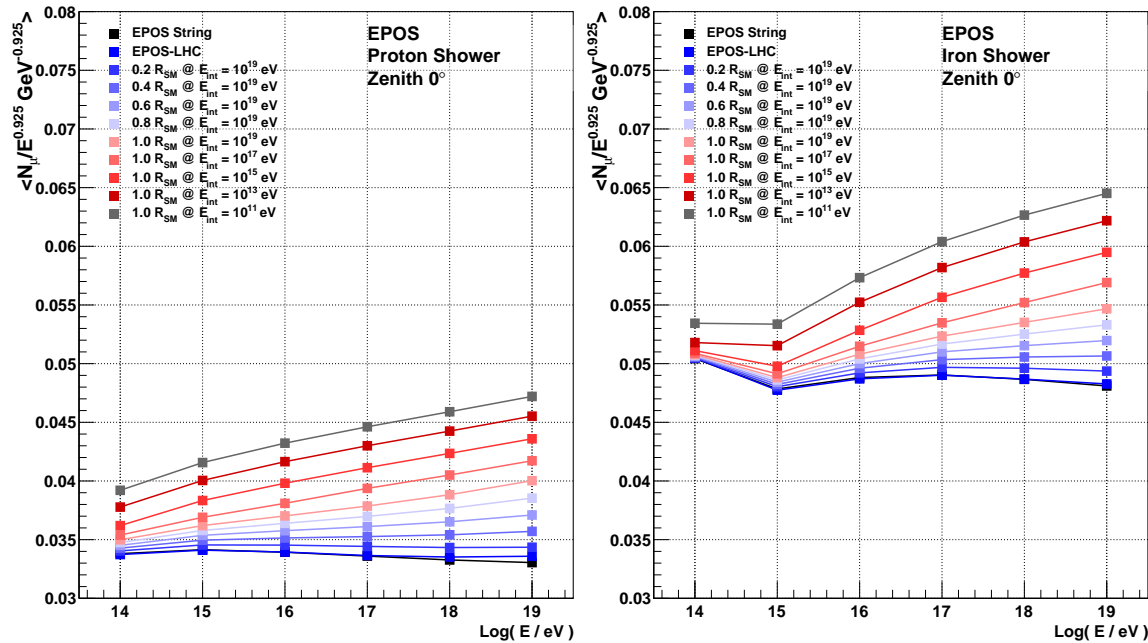


Figure 31: Muon number using R_{SM}

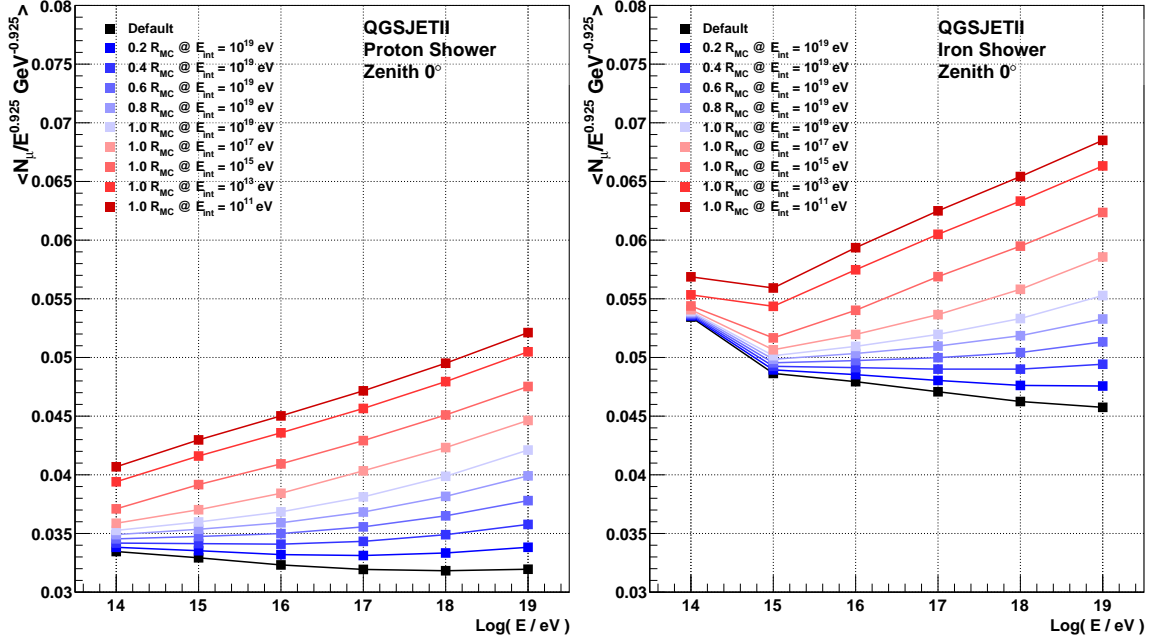


Figure 32: Muon number using R_{MC}

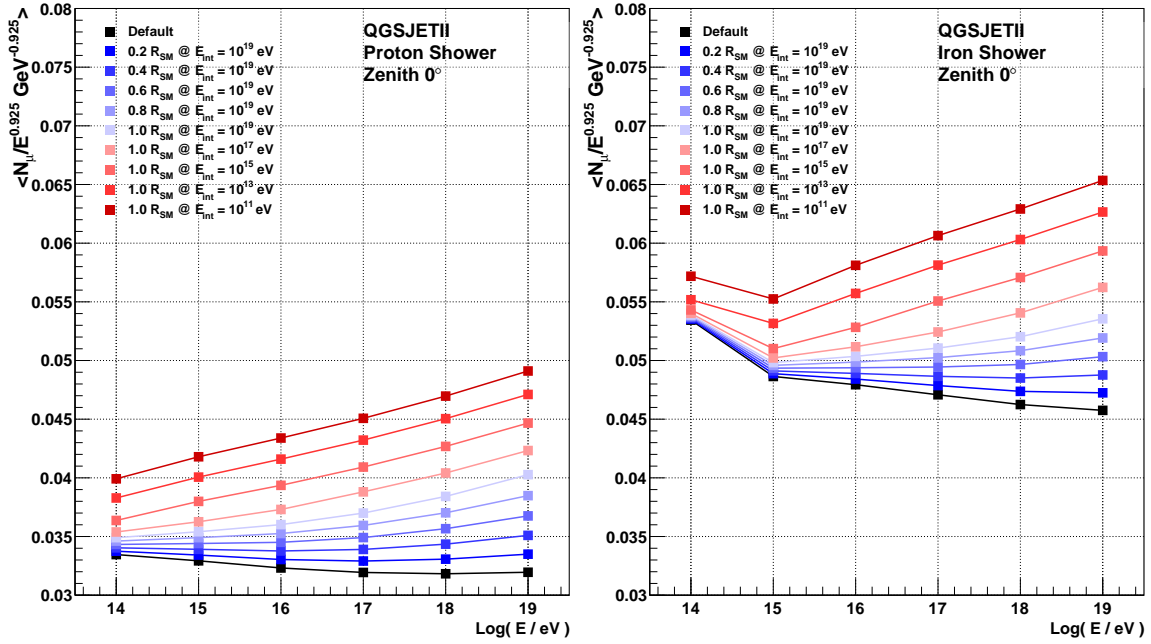


Figure 33: Muon number using R_{SM}

SIBYLL

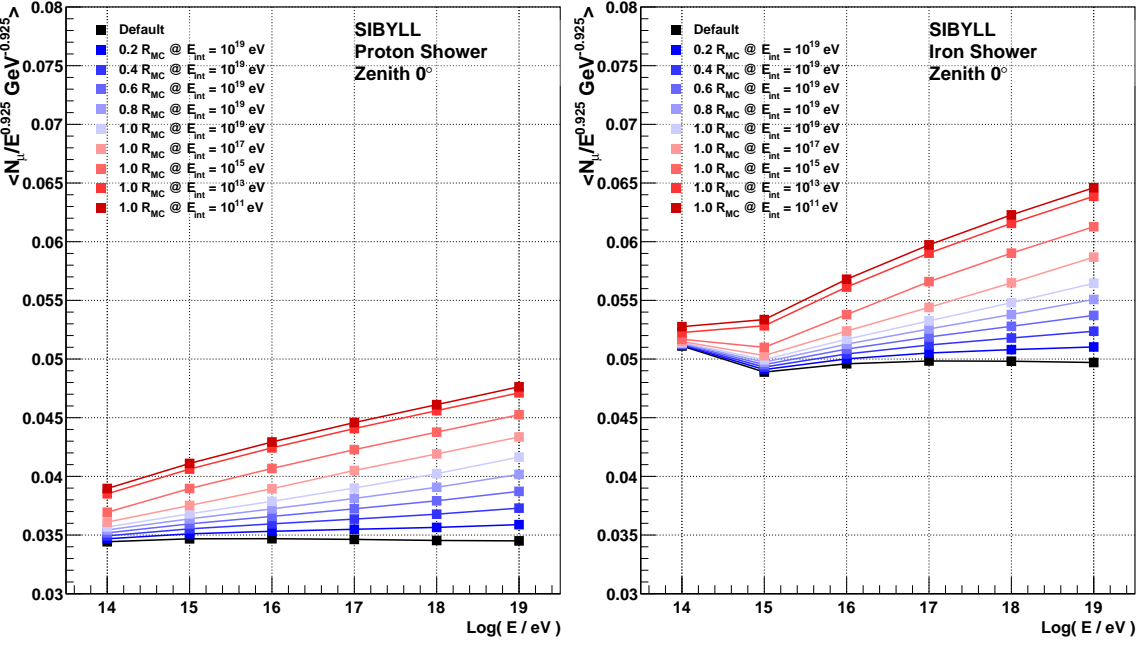


Figure 34: Muon number using R_{MC}

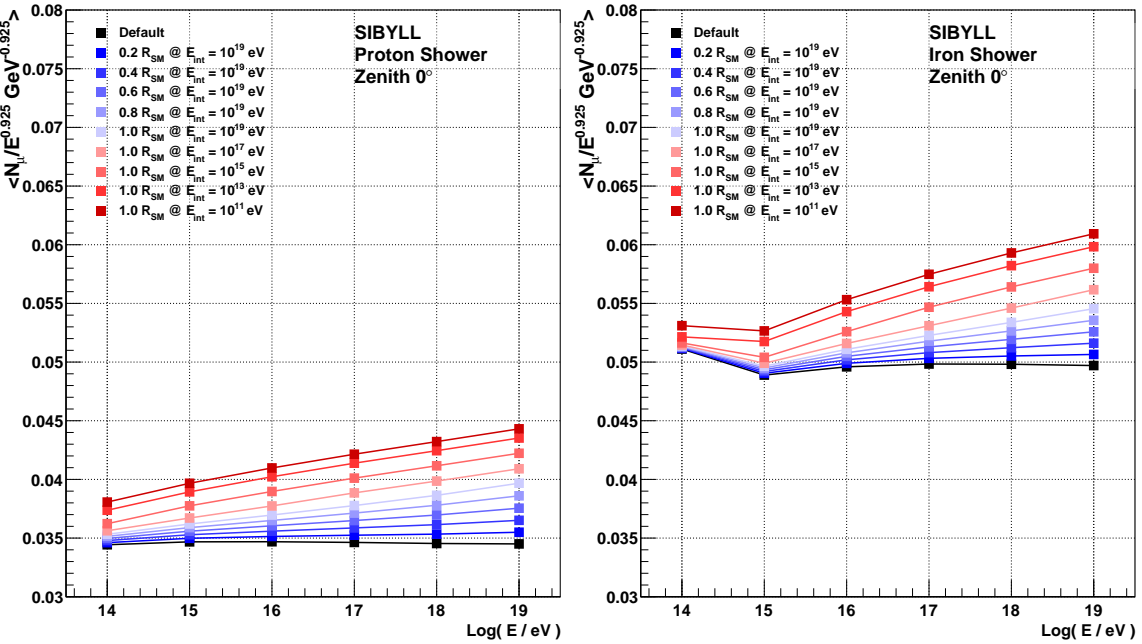


Figure 35: Muon number using R_{SM}